This full text paper was peer reviewed at the direction of IEEE Communications Society subject matter experts for publication in the ICC 2007 proceedings.

Optical Impulse Modulation for Diffuse Indoor Wireless Optical Channels

Mohamed D. A. Mohamed and Steve Hranilovic
Dept. Electrical & Computer Engineering, McMaster University
Hamilton, Ontario, L8S 4K1 Canada
Email: mdamohamed@grads.ece.mcmaster.ca, hranilovic@mcmaster.ca

***Abstract*— In this paper, power efficient signaling over indoor diffuse wireless optical channels is considered. Present-day laser diodes have pulse rates many times higher than the bandwidth of multipath distorted diffuse channels. Despite the fact that the transmitter extra degrees of freedom are not supported by the low-pass channel, they can be used to satisfy the channel non-negativity constraint. In this paper, we define optical impulse modulation (OIM) in which data are confined to the low-pass region while the high-pass region, which is distorted by the channel, is used to satisfy the channel amplitude constraints. A mathematical framework for OIM is presented, and an optimal receiver filter is designed. At a normalized delay spread of 0.2, the gain in average optical power of using decision feedback equalization (DFE) with rectangular pulse-amplitude modulation (PAM) is 4.8 dBo, while that of using the less complex unequalized OIM receiver is shown to be 4.9 dBo.**

I. Introduction

The capacity of traditional radio frequency (RF) wireless systems is limited due to the scarcity and cost of bandwidth. As a result, a new trend in wireless systems exploits the use of the optical infrared bands. Optical signals are confined to a room (by opaque boundaries), are unlicensed worldwide, and have many THz of bandwidth. Wireless optical modems are constructed from inexpensive laser diodes and photodetectors. Unlike RF channels, these devices are able to modulate and detect only the optical intensity of the carrier. These devices impact communication system design in two ways: (i) the modulated signal, which is the instantaneous intensity of the optical signal, must be non-negative, and (ii) the average transmitted optical power is given by the average signal amplitude rather than the average square amplitude.

As a result, algorithms designed for RF channels cannot be applied directly to optical channels. New modulation and coding techniques are required to design efficient communication systems. Rectangular pulse-amplitude modulation (Rect-PAM) and pulse-position modulation (Rect-PPM) were widely used over indoor optical channels [1], [2]. PPM increases the peak-to-average ratio of the modulated optical signal, and hence enhances the signal-to-noise ratio (SNR) at a cost of additional bandwidth. At low channel delay spread, PPM outperforms PAM while at high delay spread, the performance of PPM degrades quickly due to its bandwidth inefficiency [2]. To reduce the degradation of PPM performance at higher delay spreads, maximum likelihood sequence detection (MLSD) and decision feedback equalization (DFE) have been employed at a cost of higher complexity receivers [2], [3].

In this paper, a low complexity modulation scheme, *optical impulse modulation* (OIM), is defined which provides a good tradeoff between power and bandwidth efficiencies. This scheme provides high optical power gain over Rect-PAM over a wide range of channel delay spreads. A key insight of OIM is that it confines the useful information to the low-pass region of the spectrum. The higher frequency regions, which are attenuated by the channel, carry no information and are only used to satisfy the channel amplitude constraints. In Sec. II, the model of the indoor wireless optical channel is introduced. A general PAM communication system is presented in Sec. III. Optical impulse modulation (OIM) is proposed in Sec. IV, while the design of its receive filter is discussed in Sec. V. Numerical results comparing Rect-PAM, Rect-PPM and OIM are presented in Sec. VI.

II. Channel Model

The most common modulation technique used for indoor infrared links is intensity modulation (IM), where the instantaneous power, $x(t)$, of the optical carrier is modulated by the data to be transmitted. Direct detection (DD) is done via a photodetector receiver which produces an output current, $y(t)$, proportional to the received instantaneous power.

The indoor diffuse wireless optical channel suffers from multipath distortion that results from multiple reflections from room objects and walls. As a result, any transmitted pulse suffers from temporal dispersion which can be modelled as a low-pass impulse response, $h(t)$, whose bandwidth ranges from 10 to 30 MHz [1]. Experimental measurements [4], ray-tracing simulations [5], and functional modelling [6] have been used to estimate $h(t)$. In this paper, we will use the exponential functional form

$$h(t) = \frac{1}{\tau}\exp\left(\frac{-t}{\tau}\right)U(t) \leftrightarrow H(f) = \frac{1}{1+j2\pi\tau f}, \qquad (1)$$

for indoor diffuse wireless optical channels, where 2τ is the channel delay spread, and $U(t)$ is the unit step function [6]. This functional form can be used to build a simple model that predicts the power requirements of these multipath channels. Without loss of generality, the channel DC-gain, $H(0)$, is set to unity in (1).

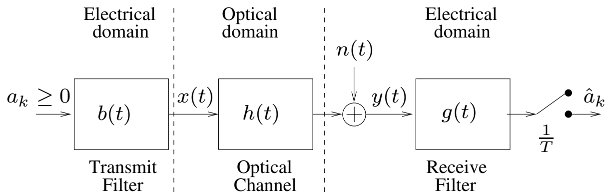

Fig. 1. Block diagram of a PAM communication system.

TABLE I

TRANSMITTER PULSE SHAPE PARAMETERS

	Rect-PAM	Sinc-PAM	OIM
pulse shape, $b(t)$	$\frac{1}{T}\text{rect}\left(\frac{t}{T}\right)$	$\frac{1}{T}\text{sinc}\left(\frac{t}{T}\right)$	$\frac{1}{\epsilon}\text{rect}\left(\frac{t}{\epsilon}\right)$
average amplitude	$1/T$	$1/T$	$1/T$
electrical energy	$1/T$	$1/T$	$1/\epsilon$

The IM/DD optical communication system can be modelled as the linear system

$$y(t) = x(t) * h(t) + n(t),$$

where $h(t)$ is the optical channel impulse response, $*$ is the convolution operator, $n(t)$ is the photodetector shot noise, and all opto-electronic conversion factors are assumed to be unity [1], [7]. Due to the intense ambient light, shot noise caused by the signal can be neglected, and the high intensity ambient-induced shot noise can be modelled as being Gaussian, white and independent of $x(t)$ [2].

Since the transmitted signal, $x(t)$, is an optical power signal, it must satisfy the constraints

$$x(t) \geq 0, \tag{2}$$

$$\mathcal{P}_t = \lim_{u\to\infty} \frac{1}{2u} \int_{-u}^{u} x(t)dt \leq \mathcal{P} \tag{3}$$

where $\mathcal{P}_t$ is the transmitted average optical power and $\mathcal{P}$ is the average optical power limit imposed by eye-safety constraints. Constraint (3) indicates that the average optical power is given by the average signal amplitude, rather than the signal square amplitude as is the case with conventional RF channels. These channel constraints prohibit the direct application of most traditional signalling schemes, and power and bandwidth efficient modulation schemes must be designed with (2) and (3) in mind.

III. PULSE AMPLITUDE MODULATION (PAM)

A PAM communication system is shown in Fig. 1. A discrete symbol sequence $\{a_k\}$ is transmitted across the channel at a rate $1/T$ by forming the transmitted signal $x(t)$ as

$$x(t) = \sum_k a_k b(t - kT), \tag{4}$$

where $b(t)$ is the transmitter pulse shape. The output of the receive filter $g(t)$ is sampled at the same rate so that an estimate $\hat{a}_k$ of a_k is obtained. Without loss of generality, the receive filter, $g(t)$, is restricted to be unit-energy throughout this paper in order not to change the total noise power at the sampler output.

The non-negativity constraint (2) can be written in terms of the symbol sequence $\{a_k\}$ and the transmitter pulse shape as

$$a_k \geq 0 \tag{5}$$

$$b(t) \geq 0. \tag{6}$$

A discrete time model for the PAM system can be developed by setting $q(t) = b(t)*h(t)*g(t)$. The equivalent discrete time impulse response of the system is $q_k = q(t_0 + kT)$, where t_0 is the sampling phase at the receiver that maximizes the cursor sample q_0. The estimate $\hat{a}_k$ is given by

$$\hat{a}_k = q_k \otimes a_k + n_k, \tag{7}$$

where $n_k = n(t) * g(t)|_{t=t_0+kT}$, and $\otimes$ is discrete time convolution.

The average transmitted optical power, $\mathcal{P}_t$, is given by

$$\mathcal{P}_t = \lim_{u\to\infty} \frac{1}{2u} \int_{-u}^{u} x(t)dt = \frac{\mu_a}{T} \int_{-\infty}^{\infty} b(t)dt, \tag{8}$$

where μ_a is the mean of $\{a_k\}$ and $\mathcal{P}_t < \mathcal{P}$ due to (3).

Table I presents the pulse shapes for PAM with rectangular and sinc pulse shapes, termed Rect-PAM and Sinc-PAM respectively, where $\text{rect}(x) = U(t + 1/2) - U(t - 1/2)$ and $\text{sinc}(x) = \sin(\pi x)/(\pi x)$. Notice that they both have the same average amplitude and electrical energy. However, the non-negativity constraint (6) prohibits the use of a large number of pulse shapes that may have better performance than rectangular pulses over inter-symbol interference (ISI) channels, such as sinc pulses, root-raised-cosine pulses, and many others. In the following section, a new modulation technique called optical impulse modulation (OIM) is proposed to enable the use of arbitrary pulse shapes over optical intensity channels.

IV. OPTICAL IMPULSE MODULATION (OIM)

The existence of very fast laser diodes, that operate in the GHz range, provides the potential for high pulse rates [7, Sec. 2.2.1]. These rates are not supported by the low-pass optical channel which has a -3 dB bandwidth of a few tens of MHz [1], [5]. Previous techniques reduced symbol rates or employed complicated equalizers in order to avoid severe multipath penalties [3], [8]. An insight of this work is that since the optical spectrum is unregulated, the extra degrees of freedom available at the transmitter due to high-speed modulators can be exploited to mitigate the channel amplitude constraints. One way of doing this is by using a set of reserved high-frequency carriers in a multiple-subcarrier modulated wireless optical system [9]. In this section, OIM is presented as an alternative approach of achieving the same goal for optical intensity PAM and PPM systems.

To conceptualize how OIM works, consider the factorization

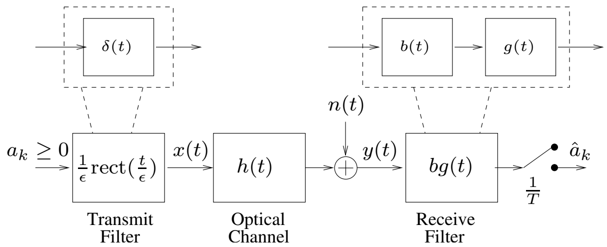

Fig. 2. OIM communication system block diagram.

of the equivalent system impulse response as follows

$$\begin{aligned} q(t) &= b(t) * h(t) * g(t) \\ &= \delta(t) * b(t) * h(t) * g(t) \\ &= \delta(t) * h(t) * bg(t), \end{aligned}$$

where $\delta(t)$ is the Dirac delta function, and $bg(t) = b(t) * g(t)$ is the combined receive filter due to $b(t)$ and $g(t)$. From the linearity of the system in Fig. 1, the factor $b(t)$ can be moved from the transmitter side to the receiver side as shown in Fig. 2. That is, the pulse shape is pushed beyond the non-negative channel into the receiver, and a combined receive filter $bg(t) = b(t) * g(t)$ is formed. As a result, the non-negativity constraint (6) on $b(t)$ is relaxed, while the non-negativity constraint (5) on the transmitted sequence $\{a_k\}$ remains. Pulse shape design is now done at the receiver, independent of the transmitter and the optical intensity amplitude constraints. This scenario allows for the use of a wider class of $b(t)$ which need not be non-negative. As in Sec. III, the filter $bg(t)$ is normalized to have unit energy in order to have the same noise power at the sampler output as previous techniques.

Practically, it is impossible to use a Dirac impulse as the transmit filter. Therefore, this impulse is approximated by a narrow pulse. For example, it can be approximated by a rectangular pulse of the form

$$\delta_\epsilon(t) = \frac{1}{\epsilon}\,\mathrm{rect}\left(\frac{1}{\epsilon}\right), \tag{9}$$

as shown in Fig. 2. Notice that a rectangular shape for $\delta_\epsilon(t)$ is not required. In fact, the specific pulse shape is immaterial as long as it is non-negative, i.e. satisfies the channel constraints and is wideband. This gives more flexibility in the transmitter filter implementation. The degradation of the performance due to this approximation is mild and is quantified in Sec. VI.

Table I shows the transmitter pulse shape for OIM. Notice that this pulse has the same average amplitude as those for Rect-PAM and Sinc-PAM, while its electrical energy is much larger for $\epsilon \ll T$. The power spectral density (PSD) of OIM is given by

$$\Phi_{OIM}(f) = \frac{\sigma_a^2}{T}\mathrm{sinc}^2(\epsilon f) + \frac{\mu_a^2}{T^2}\sum_m \mathrm{sinc}^2\left(\frac{\epsilon\, m}{T}\right)\delta\left(f - \frac{m}{T}\right) \tag{10}$$

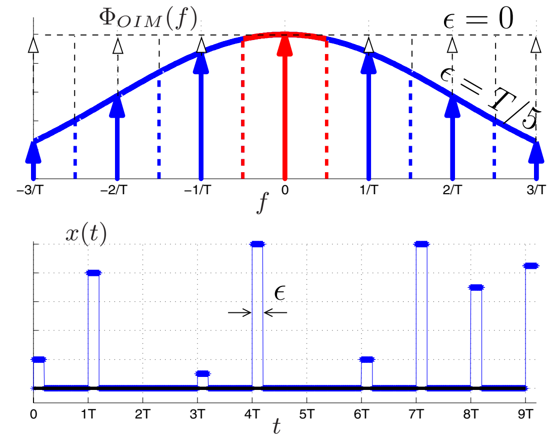

Fig. 3. The PSD and a sample time domain waveform of OIM.

where σ_a^2 is the variance of $\{a_k\}$ and the $\{a_k\}$ are assumed to be independent and identically distributed. The PSD of OIM as $\epsilon \to 0$ and $\epsilon = T/5$ are shown in Fig. 3. It is simple to show that the PSD for OIM as $\epsilon \to 0$ is a $1/T$ frequency repetition of the bandlimited Sinc-PAM spectrum. OIM uses the available out-of-band spectrum at the transmitter to satisfy the channel non-negativity constraint, while at the same time the useful information is confined to the low-pass region of the signal spectrum, as the case with Sinc-PAM. Therefore, OIM is as immune to ISI as Sinc-PAM, and at the same time satisfies the channel non-negativity constraint.

For practical ϵ, the OIM spectrum is shaped by $|\mathcal{F}\{\delta_\epsilon(t)\}|^2$, where $\mathcal{F}\{\cdot\}$ is the Fourier transform. In the case of (9), $|\mathcal{F}\{\delta_\epsilon(t)\}|^2 = \mathrm{sinc}^2(\epsilon f)$. As ϵ decreases, $|\mathcal{F}\{\delta_\epsilon(t)\}|^2$ becomes flatter and the distortion in the low-pass data bearing spectrum is small allowing for recovery using a simple low-pass filter.

V. OIM RECEIVER DESIGN

A. Whitened matched filter receiver

The optimal receiver filter is one that is matched to the received pulse. The matched filter is followed by a digital precursor equalizer to whiten the noise. The cascade of the two filters is called a whitened matched filter (WMF). Moreover, a decision feedback equalizer (DFE) can also be applied to remove postcursor ISI [10]. That is, the optimal OIM front end receive filter reduces to a filter matched to the convolution of the narrow transmit pulse (9) and the channel impulse response, $h(t)$. However, at very low channel delay spread i.e. narrow $h(t)$, the received pulse is very narrow. Consequently, the matched OIM filter is difficult to implement in practice due to the wide bandwidth and sensitivity to timing errors.

Notice also that for each channel delay spread, different WMFs and DFEs are required. Due to these difficulties, a simple receiver filter, which is independent of channel delay spread, is designed in Sec. V-B. This filter is shown to be optimal in case of flat low-pass optical channel.

B. Optimal fixed receiver filter

Since matched filtering to a wideband pulse is exceedingly difficult to implement in practice, and due to the fact that the transmitted data are confined to the low-pass region of the OIM spectrum, we restrict our attention to low-pass receiver filters. Specifically, the OIM receive filter $bg(t)$ is chosen to be a bandlimited unit-energy filter with excess bandwidth α.

Assuming that the optical channel is flat within the filter bandwidth, then in order to have no ISI as $\epsilon \to 0$, the filter $bg(t)$ is chosen to satisfy the Nyquist criterion for zero ISI. In this case, the equivalent discrete time impulse response q_k is zero for $k \neq 0$, and the discrete time system model (7) reduces to a constant channel gain:

$$\hat{a}_k = bg(0) \cdot a_k + n_k, \tag{11}$$

where $bg(0)$ is the filter cursor, and the channel DC-gain is assumed to be unity as in Sec. II. Therefore, the optimal bandlimited receive filter is the unit-energy Nyquist filter that maximizes $bg(0)$. Notice the fact that the OIM receiver can change its front end filter $bg(t)$ from one unit-energy Nyquist pulse to another independent of the transmitter and without the need to feedback any information.

Consider a general bandlimited Nyquist pulse with excess bandwidth α written as [11], [12]

$$BG(f) = \begin{cases} a, & 0 \leq |f| < \frac{1-\alpha}{2T} \\ a\,P\left(f - \frac{1-\alpha}{2T}\right), & \frac{1-\alpha}{2T} \leq |f| \leq \frac{1}{2T} \\ a\left[1 - P\left(\frac{1+\alpha}{2T} - f\right)\right], & \frac{1}{2T} < |f| \leq \frac{1+\alpha}{2T} \\ 0, & \frac{1+\alpha}{2T} < |f| \end{cases}$$

where $P(f)$ is a function satisfying $P(0) = 1$, and $a > 0$ is a scaling factor. The energy of $bg(t)$ is given by

$$\begin{aligned} \mathcal{E}_{bg} &= \int_{-\infty}^{\infty} BG^2(f)df \\ &= \frac{a^2}{T} + 4a^2 \int_0^{\alpha/(2T)} P^2(u) - P(u)du \end{aligned}$$

and the cursor is given by

$$bg(0) = \int_{-\infty}^{\infty} BG(f)df = a/T.$$

Therefore, the optimal filter can be found by solving the following optimization problem

$$\begin{aligned} \max_P \quad & a/T \\ s.t. \quad & \tfrac{a^2}{T} + 4a^2 \textstyle\int_0^{\alpha/(2T)} P^2(u) - P(u)du = 1 \end{aligned}$$

Solving the constraint for a,

$$\frac{a^2}{T^2} = \frac{1}{T + 4T^2 \int_0^{\alpha/(2T)} P^2(u) - P(u)du}. \tag{12}$$

Therefore the optimization problem reduces to

$$\begin{aligned} \min_P \quad & I(P) = \textstyle\int_0^{\alpha/(2T)} \Psi(P(u))du \\ s.t. \quad & T + 4T^2 \textstyle\int_0^{\alpha/(2T)} P^2(u) - P(u)du \; > \; 0, \end{aligned}$$

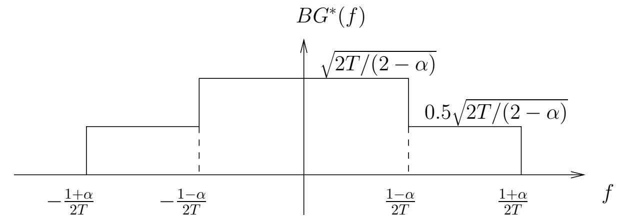

Fig. 4. Optimal double-jump receive filter for OIM.

where $\Psi(P) = P^2 - P$. Notice that the requirement that $P(0) = 1$ is immaterial in evaluating the integral $I(P)$. The unconstrained problem is solved by putting $P(u) = P^*(u) + \epsilon\,\eta(u)$, where $P^*(u)$ is the optimal solution and $\eta(u)$ is an arbitrary trajectory. Therefore,

$$I(\epsilon) = \int_0^{\alpha/(2T)} \Psi(P^*(u) + \epsilon\,\eta(u))du.$$

If P^* minimizes $I(P)$, then $I(\epsilon)$ must have a minimum at $\epsilon = 0$ for all trajectories $\eta(u)$. That is

$$V_I = \left.\frac{dI}{d\epsilon}\right|_{\epsilon=0} = 0,$$

where V_I is the first variation of the integral I along $P^*(u)$ [13]. Therefore,

$$\begin{aligned} V_I &= \left.\int_0^{\alpha/(2T)} \frac{d\Psi}{dP}\frac{dP}{d\epsilon}du\right|_{\epsilon=0} \\ &= \int_0^{\alpha/(2T)} (2P^*(u) - 1)\,\eta(u)du \end{aligned}$$

For V_I to vanish for all $\eta(u)$, we must have $(2P^*(u) - 1) = 0$ which yields

$$P^*(u) = \frac{1}{2}.$$

This value of P satisfies the constraint of the optimization problem and hence is optimal. Substituting by $P^*(u)$ into (12), $a^2 = 2T/(2-\alpha)$. As a result, the optimal filter is given by the unit-energy double-jump pulse

$$BG^*(f) = \begin{cases} \sqrt{2T/(2-\alpha)} & 0 \leq |f| < \frac{1-\alpha}{2T} \\ \frac{1}{2}\sqrt{2T/(2-\alpha)} & \frac{1-\alpha}{2T} \leq |f| \leq \frac{1+\alpha}{2T} \\ 0 & \frac{1+\alpha}{2T} < |f| \end{cases}$$

as shown in Fig. 4.

The cursor of the optimal receive filter is given by

$$bg^*(0) = \frac{1}{\sqrt{T}}\sqrt{\frac{2}{2-\alpha}}. \tag{13}$$

On the other hand, consider Rect-PAM where the receive filter is a unit-energy filter matched to the rectangular transmit filter. We term this case *unequalized* Rect-PAM, and it is a conventional scenario used in previous studies [1], [2]. For a flat channel, this system reduces to

$$\hat{a}_k = \frac{1}{\sqrt{T}} \cdot a_k + n_k, \tag{14}$$

where $1/\sqrt{T}$ is the channel gain calculated using Table I.

For the same sequence $\{a_k\}$ on a flat channel for $\epsilon \to 0$, the average optical power gain of OIM over Rect-PAM is found by comparing (11), (13) and (14) to give

$$\gamma = \sqrt{\frac{2}{2-\alpha}} \tag{15}$$

Notice that this gain is increasing in α and reaches a maximum of 1.5 dBo at $\alpha = 1$.

Pulse-position modulation (L-PPM) is coded PAM in which $\log_2(L)$ bits are encoded by transmitting a single pulse in one of L successive chips each of duration T_c. OIM can be applied to PPM in the same way it was applied to PAM. Numerical results for both schemes are presented in Sec. VI.

VI. Numerical Results

Figure 5 presents a plot of the normalized optical power required to achieve a bit error rate (BER) of 10^{-6} versus the normalized channel delay spread, $2\tau/T$, for unequalized Rect-PAM and OIM with double-jump receiver when $a_k \in \{0, 1\}$, i.e, on-off keying (OOK). The optical power is normalized to the power required by Rect-PAM OOK over a flat channel.

The effect of non-zero values of ϵ is quantified in Fig. 5 by taking $\epsilon = T/2, T/5, T/10^6$. The optical power curve at $\epsilon = T/5$ nearly coincides with that at $\epsilon = T/10^6$, which indicates a fast convergence of the power curves in the limit $\epsilon \to 0$. For a typical indoor diffuse channel, the bandwidth is 10 to 30 MHz [1]. Therefore, using $\epsilon = T/5$ implies a pulse rate from 50 to 150 MHz, which is far below the rates available in present day laser diodes.

The gain in optical power of OIM (15) at zero delay spread for $\alpha = 0$ and $\alpha = 1$ is evident in Fig. 5. Notice that the gain is higher at larger normalized delay spreads. For instance, in Fig. 5 with $\alpha = 0$, the gain vanishes at zero delay spread as suggested by (15), and increases gradually as the channel delay spread increases. This is attributed to the fact that the useful information is confined to the low-pass region of the OIM spectrum as shown in Fig. 3, while the spectrum of Rect-PAM is wideband. Therefore, OIM shows better immunity to the channel multipath dispersion. For example, at a normalized channel delay spread of 0.2, the gain of OIM over Rect-PAM is 3.2 dBo at $\alpha = 0$, and 4.9 dBo at $\alpha = 1$.

Figure 6 presents a comparison of OOK Rect-PAM and OIM when a WMF is employed as well as the case when a DFE is employed. For a flat channel, i.e., $2\tau/T \to 0$, the WMF is a filter matched to the transmitted pulse. In this case, the channel gain is equal to the square root of the transmit pulse energy. Using the values of pulse energies from Table I, equalized OIM achieves a gain of $\sqrt{T/\epsilon}$ in optical power over equalized Rect-PAM, at zero delay spread. As a result, the gain of OIM over Rect-PAM with matched receive filters at low delay spreads increases as ϵ decreases. As mentioned earlier, despite this high gain at low delay spread, matched filtering to a narrow transmitted pulse is difficult to implement in practice. Thus, the use of a WMF for OIM is practical only at moderate to high delay spreads. In the case of a wide

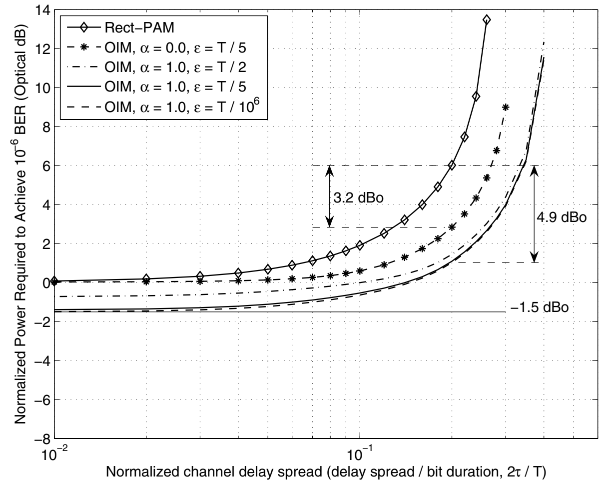

Fig. 5. Normalized optical power required by unequalized OOK Rect-PAM and OIM with double-jump receiver to achieve BER=10^{-6}.

TABLE II
Optical power gain over unequalized OOK Rect-PAM for $2\tau/T = 0.2$. For OIM, $\epsilon = T/5$ is used.

	OIM, $\alpha = 1$ double-jump	Rect-PAM WMF	Rect-PAM DFE	OIM WMF	OIM DFE
Gain (dBo)	4.92	1.14	4.76	5.4	5.99

bandwidth channel, the OIM receiver can switch its front end filter to the double-jump filter (Fig. 4), without the need to feedback any information to the transmitter. At higher delay spreads, the use of a WMF and DFE greatly improves the performance of Rect-PAM over the unequalized case. Note that the performance of OIM with WMF and DFE remains better than a comparable Rect-PAM, however, the incremental gain in using the equalizer is less for OIM versus Rect-PAM. Notice also that the performance of equalized OIM is relatively insensitive to the choice of ϵ so long as it is chosen small enough, i.e., $\epsilon \leq T/5$.

The gain in optical power over unequalized OOK Rect-PAM is listed in Table II for different PAM schemes at a normalized channel delay spread of 0.2. The gain of OIM with double-jump receiver is slightly greater than that of Rect-PAM with WMF and DFE receiver. That is, OIM with a single, simple low-pass receive filter provides slightly better performance than the more complex receiver Rect-PAM with WMF and DFE. Notice that in addition to the lower complexity, a single double-jump receive filter is used for OIM for all delay spreads, while different WMFs and DFEs are required for each channel delay spread in the case of Rect-PAM.

The normalized optical power is plotted in Figs. 7 and 8 for unequalized and equalized PPM respectively. Similar optical power gains, to those achieved with PAM systems, are achieved by OIM-PPM in both the unequalized and WMF scenarios. A DFE can also be applied to PPM at the chip-rate

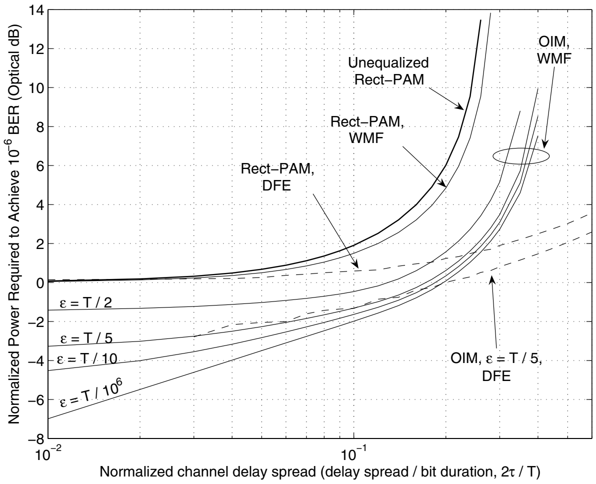

Fig. 6. Normalized optical power required by equalized OOK Rect-PAM and OIM to achieve BER=10^{-6}.

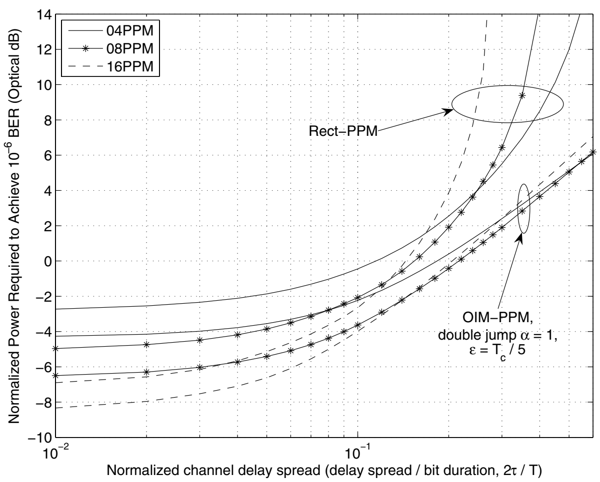

Fig. 7. Normalized optical power required by unequalized Rect-PPM and OIM-PPM to achieve BER=10^{-6}.

or the symbol-rate. The performance of these DFE systems is examined in [3] on measured indoor channels.

VII. Conclusion

Optical impulse modulation is a general scheme to transmit a non-negative discrete sequence over an optical intensity channel. It can be used with all PAM-based modulation techniques such as PPM, differential PPM (DPPM) [14], and multiple PPM (MPPM) [15] as well as many others. In simulations, the average optical power requirement for OOK using OIM is less than that required by Rect-PAM employing a complex WMF and DFE.

The design of OIM exploits the wide unregulated bandwidth available in indoor wireless optical channels. This unique feature of these channels enables the system designer to exploit the excess degrees of freedom at the transmitter to satisfy amplitude constraints while transmitting bandwidth efficient pulses. Thus, OIM is able to simultaneously achieve high

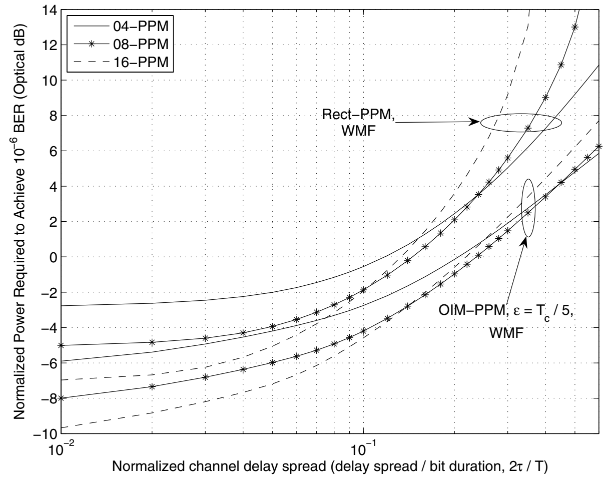

Fig. 8. Normalized optical power required by precursor equalized Rect-PPM and OIM-PPM to achieve BER=10^{-6}.

bandwidth and power efficiencies.

References

[1] J. M. Kahn and J. R. Barry, "Wireless infrared communications," *Proc. IEEE*, vol. 85, no. 2, pp. 263–298, Feb. 1997.

[2] M. D. Audeh, J. M. Kahn, and J. R. Barry, "Performance of pulse-position modulation on measured non-directed indoor infrared channels," *IEEE Trans. Commun.*, vol. 44, no. 6, pp. 654 – 659, June 1996.

[3] ——, "Decision-feedback equalization of pulse-position modulation on measured nondirected indoor infrared channels," *IEEE Trans. Commun.*, vol. 47, no. 4, pp. 500 – 503, Apr. 1999.

[4] J. M. Kahn, W. J. Krause, and J. B. Carruthers, "Experimental characterization of non-directed indoor infrared channels," *IEEE Trans. Commun.*, vol. 43, no. 234, pp. 1613–1623, Feb./Mar./Apr. 1995.

[5] J. R. Barry, J. M. Kahn, W. J. Krause, E. A. Lee, and D. G. Messerschmitt, "Simulation of multipath impulse response for indoor wireless optical channels," *IEEE J. Sel. Areas Commun.*, vol. 11, no. 3, pp. 367–379, Apr. 1993.

[6] J. B. Carruthers and J. M. Kahn, "Modeling of nondirected wireless infrared channels," *IEEE Trans. Commun.*, vol. 45, no. 10, pp. 1260–1268, Oct. 1997.

[7] S. Hranilovic, *Wireless Optical Communication Systems*. Springer, 2004.

[8] G. W. Marsh and J. M. Kahn, "Performance evaluation of experimental 50-Mb/s diffuse infrared wireless link using on-off keying with decision-feedback equalization," *IEEE Trans. Commun.*, vol. 44, no. 11, pp. 1496–1504, Nov. 1996.

[9] W. Kang and S. Hranilovic, "Optical power reduction for multiple-subcarrier modulated indoor wireless optical channels," in *Proc. IEEE Int. Conf. Commun.*, vol. 6, Istanbul, Turkey, June 2006, pp. 2743–2748.

[10] E. A. Lee and D. G. Messerschmitt, *Digital Communication*, 2nd ed. Kluwer Academic Publishers, Jan. 1994.

[11] H. Nyquist, "Certain topics in telegraph transmission theory," *Trans. AIEE*, vol. 47, pp. 617-644, Feb. 1928.

[12] N. C. Beaulieu and M. O. Damen, "Parametric construction of Nyquist-I pulses," *IEEE Trans. Commun.*, vol. 52, no. 12, pp. 2134–2142, Dec. 2004.

[13] G. A. Bliss, *Lectures on the Calculus of Variations*. The University of Chicago Press, 1946.

[14] D. Shiu and J. M. Kahn, "Differential pulse-position modulation for power-efficient optical communication," *IEEE Trans. Commun.*, vol. 47, no. 8, pp. 1201–1210, Aug. 1999.

[15] H. Sugiyama and K. Nosu, "MPPM: A method for improving the band-utilization efficiency in optical PPM," *IEEE J. Lightwave Tech.*, vol. 7, no. 3, pp. 465–472, Mar. 1989.